33rd Annual International Conference of the IEEE EMBS
Boston, Massachusetts USA, August 30 - September 3, 2011

Automated detection of the carotid artery wall in longitudinal B-mode images using active contours initialized by the Hough transform

A. I. Matsakou, S. Golemati, *Member*, *IEEE*, J. S. Stoitsis, *Member*, *IEEE*, and K. S. Nikita, *Senior Member*, *IEEE*

***Abstract*—In this paper, a fully automatic active-contour-based segmentation method is presented, for detecting the carotid artery wall in longitudinal B-mode ultrasound images. A Hough-transform-based methodology is used for the definition of the initial snake, followed by a gradient vector flow (GVF) snake deformation for the final contour detection. The GVF snake is based on the calculation of the image edge map and the calculation of GVF field which guides its deformation for the estimation of the real arterial wall boundaries. In twenty cases there was no significant difference between the automated segmentation and the manual diameter measurements. The sensitivity, specificity and accuracy were 0.97, 0.99 and 0.98, respectively, for both diastolic and systolic cases. In conclusion, the proposed methodology provides an accurate and reliable way to segment ultrasound images of the carotid artery.**

Keywords— **Carotid artery wall, B-mode ultrasound, Segmentation, Hough transform, Gradient vector flow snake.**

I. Introduction

ULTRASOUND imaging of the carotid artery is widely used in the diagnosis of atherosclerosis, because it provides valuable information about the arterial wall and plaque morphology. Measurements of the lumen diameter are conventionally obtained by manually tracing the wall-lumen interface. In practice this procedure is time consuming and extremely subjective because it depends on the training, the experience and the expertise of the observer. The manual measurements suffer therefore from considerable inter- and intra- observer variability [1]. To address these problems, advanced computerized image segmentation methods have been developed for accurate measurements of the carotid artery. Previous studies on segmentation of the carotid artery wall have proposed the application of inflating balloon models [1], dynamic programming [1], deformable models [3] and active contours [4], [5]. Among them, active contour models have been proved to be more effective.

The methods in the previously mentioned studies are effective, but they are either automatic with high complexity and computational cost [1] or semiautomatic due to user interaction in the initialization step [1]–[5]. To overcome these drawbacks, attempts have been made to implement fully automatic detection methods with low complexity and computational cost either by using known image transforms or by automating the initialization step of the active contour methods [6], [7]. Specifically, the Hough transform (HT) was used to automatically segment the arterial wall from ultrasound images [8], [9]. Golemati *et al.* [8] proposed a fully automatic method to extract the arterial wall in the form of straight lines and circles, for longitudinal and transverse ultrasound image sequences of the carotid artery, respectively. Despite the good performance of the method, the HT failed to match the random shape of the arterial wall. However, it can be used to provide an initial contour estimation for the active contour method [10]. Stoitsis *et al.* [10] used HT combined with an active-contour-based method to automatically detect the arterial wall boundaries in transverse sections of the carotid artery.

The objective of this paper was to investigate the possibility of combining two segmentation techniques, the HT and the gradient vector flow (GVF) snake, in an attempt to improve the snake initialization method and implement an open GVF snake deformation to automatically detect the carotid artery wall from longitudinal B-mode ultrasound images. The method relies on the use of the HT transform methodology described in [8] to estimate the initial snake contour, which is then processed and deformed according to the GVF snake model [11]. The results of the method are validated in real ultrasound images through comparisons with measurements obtained from manually delineated wall boundaries.

II. Material and Methods

A. Recording of Ultrasound Images

A total of 10 systolic and 10 diastolic B-mode longitudinal ultrasound images were selected from image sequences of the common carotid artery. The image sequences were recorded from young subjects (ages: 25-32 years) with normal, i.e. non-stenotic, carotid arteries. For each subject, image sequences were acquired with an ATL (Advanced Technology Laboratory) Ultramark 4 Duplex scanner (Philips Medical Systems, Bothell, WA, USA) and a high resolution 7.5MHz linear array scan head. Scanner

Manuscript received April 15, 2011.

A. I. Matsakou, J. S Stoitsis and K. S. Nikita are with the Department of Electrical and Computer Engineering, National Technical University of Athens, Athens 15780, Greece (e-mail: kmatsakou@biosim.ntua.gr).

S. Golemati is with the Medical School, National Kapodistrian University of Athens, Athens 10675, Greece (e-mail: sgolemati@med.uoa.gr).

settings were constant for all measurements at the following values: dynamic range 60dB; 2-D gray map linear; persistence low; frame rate high. The gain, which is a subjective parameter in scanner settings, was adjusted so that the blood and adventitia fulfilled the following criteria: (a) the blood was dark and with uniform echogenicity and (b) the adventitia was thick, bright and with uniform echogenicity. The sequences were recorded at a rate of 25 frames/s for approximately 3 seconds, corresponding to 2-3 cardiac cycles, during breath holding.

B. Detection of the Arterial Wall Boundaries

In all images, the average gray-scale median (GSM) of the pixels in the blood ranged between 0 and 5, whereas that of the adventitia between 180 and 190. According to widely accepted specifications for normalization of B-mode ultrasound images of the carotid artery, images with these GSM values are considered normalized and therefore no further standardization was performed. It is recommended that the methodology described below is applied to normalized ultrasound images to minimize variability introduced by different equipment, operators and gain settings and facilitate tissue comparability.

The proposed methodology includes the following steps, presented in more detail below: (1) estimation of the initial arterial wall contour using the HT methodology described in [8], (2) calculation of the image edge map, (3) calculation of the GVF field using the image edge map calculated in the previous step, and (4) deformation of the initial contour based on the GVF field.

Initial arterial wall estimation using HT. The HT technique allows the automatic extraction of straight lines representing the wall-lumen boundaries in longitudinal images [8]. HT is applied on the $N_1 \times N_2$ binary image, resulting from the edge detection step, and transforms it to a parametric matrix $P(r,\theta)$, where (r,θ) are the polar coordinates of a straight line of the form $r = x\cos\theta + y\sin\theta$, and $0 \le r \le \sqrt{N_1^2 + N_2^2}$ and θ are the distance from the upper left corner of the image and its angle with the x-axis, respectively. For every binary edge image pixel and for any angle $75° \le \theta \le 105°$, the matrix element corresponding to the coordinates (x,y) is increased by the magnitude of the gradient. The main steps of the technique, described in detail in [8], include: (1) reduction of image area; this is important because it minimizes the possibility to detect unwanted structures, and also reduces the computational cost and the time required for the segmentation, (2) image pre-processing, (3) edge detection, (4) application of HT, and (5) selection of dominant lines.

Calculation of the image edge map. This step includes the processing of the reduced image that resulted from the HT methodology in order to estimate the gradient field of the image edge map. The processing step includes the following tasks: (1) calculation of the gradient field by applying the gradient operator, (2) thresholding the gradient field to remove the small gradient values due to speckle noise and to enhance the strong edges, (3) morphological closing and opening of the image and smoothing of the gradient field, using a symmetric Gaussian low-pass filter with kernel size 7×7 and $\sigma_x=\sigma_y=1$, and (4) gradient operator application to estimate the image edge map. The edge map derived from the image has large values near the edges and zero value in homogeneous regions of the image.

Calculation of the GVF field. The GVF field, defined by $\mathbf{v}(x,y) = [u(x,y), v(x,y)]$, was calculated to minimize the energy functional [11]:

$$E = \iint \mu \cdot (u_x^2 + u_y^2 + v_x^2 + v_y^2) + |\nabla f|^2 |\mathbf{v} - \nabla f|^2 \, dxdy \quad (1)$$

where f is the image edge map, calculated in the previous step, $\nabla f = (f_x, f_y)$ is the gradient of the image edge map, and μ is a regularization parameter that should be set according to the amount of noise present in the image (more noise, increased μ) [11]. A value of 0.2 was used for μ in this study.

Minimizing the energy functional of equation (1) gives rise to the following two independent Euler equations [11]:

$$\begin{aligned} \mu\nabla^2 u - (u - f_x)(f_x^2 + f_y^2) = 0 \\ \mu\nabla^2 v - (v - f_y)(f_x^2 + f_y^2) = 0 \end{aligned} \quad (2)$$

where ∇^2 is the Laplacian operator. The GVF field can be found solving equations (2).

Deformation of the initial contour based on the GVF field. The initial curve defined in the initialization step is considered to be a snake that uses the GVF field as its external force. This GVF snake is defined as the parametric curve $\mathbf{x}(s) = [x(s), y(s)]$ solving the dynamic equation [11]:

$$\mathbf{x}_t(s,t) = \alpha \cdot \mathbf{x}'' - \beta \cdot \mathbf{x}'''' + k \cdot \mathbf{v}(\mathbf{x}) \quad (3)$$

where $\mathbf{x}$ is treated as a function of time t and space s, α and β are the tension and rigidity parameters of the snake, respectively, and k controls the extent to which the GVF field affects the deformation of the curve. The values $\alpha = 0.05$, $\beta = 0$, and $k = 1$ were used in this study.

The dynamic equation (3) is solved by discretization and iteration, in identical fashion to the traditional snake. The iterative equations for the snake deformation of the initial curve are [11]:

$$\begin{aligned} \mathbf{x}_t &= (\mathbf{A} + \gamma \cdot \mathbf{I})^{-1} (\gamma \cdot \mathbf{x}_{t-1} + k \cdot \mathbf{u}(\mathbf{x}_{t-1}, \mathbf{y}_{t-1})) \\ \mathbf{y}_t &= (\mathbf{A} + \gamma \cdot \mathbf{I})^{-1} (\gamma \cdot \mathbf{y}_{t-1} + k \cdot \mathbf{v}(\mathbf{x}_{t-1}, \mathbf{y}_{t-1})) \end{aligned} \quad (4)$$

where $\mathbf{x}$ and $\mathbf{y}$ are the coordinates' vectors of the points of the curve, $\gamma = 1/\Delta t$ the step size of the iteration, $\mathbf{I}$ a diagonal identity matrix and $\mathbf{A}$ is a pentadiagonal matrix with incorporated boundary conditions for the open-ended snake used for the longitudinal images. After each iteration, the snake is dynamically re-parameterized to maintain the point separation within 0.5-1.5 pixels [12].

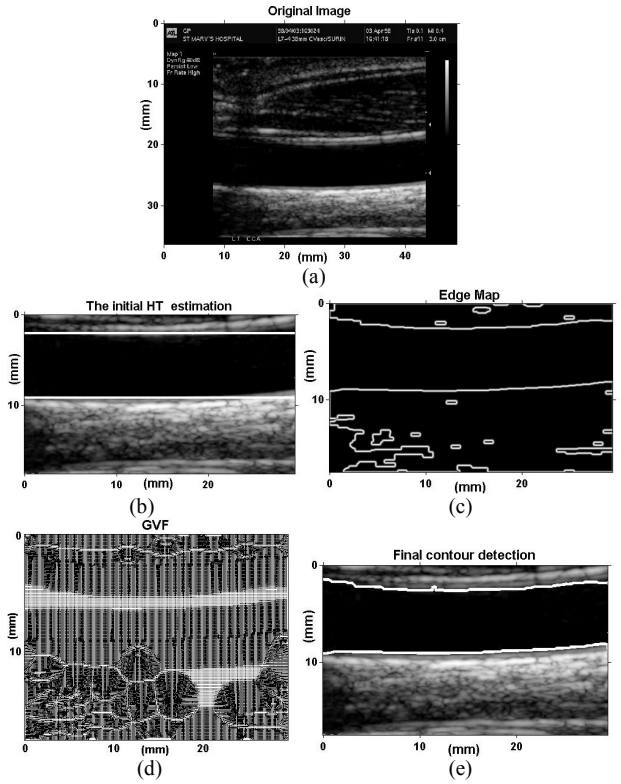

Fig. 1. Example of the results of the application of each step of the proposed method: (a) original image, (b) initial arterial wall estimation using HT, (c) the image edge map, (d) the gradient flow field and (e) final contour after deformation based on the GVF field.

C. *Validation methodology*

The parameters D_{mean}, D_{median}, D_{min}, and D_{max} were computed, corresponding to the mean, median, minimum and maximum, respectively, vertical distances between the anterior and posterior wall contours obtained from the automated and manual segmentations. The range R of the measurements was calculated as the difference between D_{max} and D_{min}.

The Wilcoxon matched pairs rank sum test was used to identify whether significant differences existed between the contours obtained from the manual and the automated segmentation procedures, at $p<0.05$.

To evaluate the performance of the proposed method, the automatically defined wall-lumen boundaries were compared with the boundaries defined manually by an expert physician. The area corresponding to automatic segmentation is the surface defined by the two random-shaped boundaries corresponding to the anterior and posterior walls (calculated from the deformation of the snake) and the two lines connecting the previous ones at their left and right edges. The area corresponding to the manual segmentation is the surface defined by the two random-shaped boundaries corresponding to the anterior and posterior walls (delineated by the physician) and the two lines connecting their left and right edges.

Receiver operating characteristics (ROC) analysis was used to assess the sensitivity, specificity, and accuracy of the method calculated as described in [8], after estimating the number of true positive, true negative, false positive and false negative pixels. True positive pixels are the pixels that automatic and manual segmentation identified as segmented; true negative are the pixels that automatic and manual segmentation did not identified as segmented; false positive are the pixels that automatic segmentation identified as segmented, but manual segmentation did not; and false negative pixels are the pixels that manual segmentation identified as segmented but automatic segmentation did not. Sensitivity, specificity and accuracy were estimated separately for the images corresponding to diastole and systole.

III. Results

Figure 1 shows an example of the application of each step of the proposed method in a longitudinal section of the carotid artery. It can be easily observed that, compared to the initial HT-transform-based boundary (Fig. 1(b)), the result of the present method (Fig. 1(e)) provides a better estimation of the random shape of the arterial wall.

Table I shows the diastolic and systolic diameter values (average values $\pm$ std) for the manually and automatically segmented images and the corresponding p-values. The automated measurements had a significantly larger range of values than the manual ones (p-value = 0.03 for diastole and p-value = 0.005 for systole), while the mean and median values were underestimated in both diastolic and systolic cases. However, no statistically significant difference was found between manual and automated measurements, with an exception for the underestimation of the diastolic D_{min} measurement (p-value = 0.003).

The ROC analysis results for the sensitivity, specificity and accuracy (average values $\pm$ std) are presented in Table II. For comparison reasons, the corresponding results of the HT segmentation methodology, applied in [8], are also presented. It can be seen that the ROC indices of the method are particularly high with sensitivity values being slightly lower compared to the two other indices.

The time needed to detect the two wall boundaries in a single image did not exceed 40s using a 3.00 GHz personal computer, indicating the low computational cost of the method.

IV. Discussion

The proposed methodology provides a fully automatic segmentation of the arterial lumen of the carotid artery in longitudinal ultrasound images. Its main advantage is the HT-based initialization step, which overcomes the limitations of the user-initialized active contour methods. In a small dataset of normal subjects the method exhibited high sensitivity, specificity and accuracy.

The large range of values on the diameter metrics showed that the automated measurements are not very concentrated, which may be due to the limited number of images used in this study. In the case of the diastolic D_{min} measurement, the

TABLE I
DIAMETER METRICS (AVERAGE VALUES ± STD), IN MM, OF MANUAL AND AUTOMATED SEGMENTATION MEASUREMENTS

	Diastole			Systole		
	Manual	Automated	p-value	Manual	Automated	p-value
D_{mean}	6.04 ± 0.07	6.00 ± 0.09	0.34	6.77 ± 0.03	6.73 ± 0.07	0.68
D_{median}	6.04 ± 0.04	5.97 ± 0.06	0.30	6.76 ± 0.05	6.71 ± 0.03	0.52
D_{min}	5.81 ± 0.04	5.57 ± 0.03	0.003	6.46 ± 0.08	6.26 ± 0.06	0.15
D_{max}	6.37 ± 0.03	6.78 ± 0.13	0.08	7.09 ± 0.06	7.41 ± 0.04	0.11
R	0.56 ± 0.05	1.21 ± 0.13	0.03	0.63 ± 0.08	1.15 ± 0.07	0.005

significant underestimation noted could be caused by the speckle noise and the choice of parameter values in the morphological closing and opening tasks during the calculation of the edge map.

In terms of the ROC indices, the methodology seems superior compared to those of other studies. Specifically, it is shown in Table II that in comparison to the corresponding results of the HT methodology [8], all validation indices were increased with the application of the HT-initialized GVF methodology. Ceccarelli *et al*. [6] reported a percentage of correct detection of the intima-media complex higher than 84.78% using automatically initialized active contours. Cheng *et al*. [4] also detected the intimal and adventitial layers of the carotid wall using a semi-automatic active-contour-based method, with mean square errors of 0.6510 and 0.4022, respectively. The application of a semi-automatic balloon-model-based approach [2] for the segmentation of three-dimensional (3D) carotid images showed agreement with the manual segmentation at 65% of the 3D-mesh points. However, direct comparison with the previous studies is difficult and cannot lead to safe conclusions, because the image samples, the applications, and the validation criteria are different.

It should be noted that the lower sensitivity values indicate that the method is more efficient for the detection of true negative pixels than for true positive pixels. This may be due to the quality of the images and also the fact that in the tested images the percentage of true negative pixels is quite high. Furthermore, the parameter values used in the image edge map calculation can affect the performance of the methodology and their selection should be made carefully. In this paper, the values used were selected according to the image characteristics based on experiments performed on a small set of data.

TABLE II
AVERAGE VALUES (± STD) OF SENSITIVITY, SPECIFICITY AND ACCURACY OF THE HT AND HT–INITIALIZED GVF METHODOLOGIES

	HT	HT-initialized GVF
Sensitivity		
Diastole	0.96 ± 0.03	0.971 ± 0.006
Systole	0.97 ± 0.02	0.976 ± 0.006
Specificity		
Diastole	0.97 ± 0.02	0.992 ± 0.002
Systole	0.98 ± 0.01	0.993 ± 0.002
Accuracy		
Diastole	0.97 ± 0.01	0.985 ± 0.001
Systole	0.98 ± 0.03	0.988 ± 0.003

V. CONCLUSION

In this paper a simple and accurate method was suggested, that can be used for the segmentation of the carotid artery wall in longitudinal B-mode ultrasound images. The initial estimate of the contour is derived from the application of the HT methodology and the contour is then deformed using GVF snakes. The method will be further evaluated on larger datasets, including images of atherosclerotic vessels.

REFERENCES

[1] I. Wendelhag, Q. Liang, T. Gustavsson, and J. Wikstrand, "A new automated computerized analyzing system simplifies reading and reduces the variability in ultrasound measurement of intima media thickness," *Stroke* vol. 28, no. 2, pp. 2195–2200, Nov. 1997.

[2] J.D. Gill, H.M. Ladak, D.A. Steinman and A. Fenster, "Accuracy and variability assessment of a semiautomatic technique for segmentation of the carotid arteries from three-dimensional ultrasound images," *Med Phys*, vol. 27, no.6, pp. 1333–1342, Jun. 2000.

[3] F. Mao, J. Gill, D. Downey and A. Fenster, "Segmentation of carotid artery in ultrasound images: Method development and evaluation technique. *Med Phys*, vol. 27, no. 8, pp. 1961 – 1970, Aug. 2000.

[4] D.C. Cheng, A. Schmitdt-Truckäss, K.S. Cheng and H. BurkHardt, "Using snakes to detect the intimal and adventitial layers of the common carotid artery wall in sonographic images," *Comput Meth Prog Bio*, vol. 67, no. 1, pp. 27 – 37, Jan. 2002.

[5] C.P. Loizou, C.S. Pattichis, M. Pantziaris, T. Tyllis, and A. Nicolaides, "Snakes based segmentation of the common carotid artery intima media," *Med Bio Eng Comput*, vol. 45, no. 1, pp. 35–49, Jan. 2007.

[6] M. Ceccarelli, N. De Luca, and A. Morganella, "An active contour approach to automatic detection of the intima-media thickness," in *2006 Proc. IEEE Int. Conf. Acoustics, Speech and Signal Processing*. ICASSP 2006, vol. 2, pp. 709–712.

[7] P. Turcza, T. P. Zieliński, A. Kwater, and T. Grodzicki, "Computationally efficient algorithm of the intima-media thickness of the common carotid artery," *Procedia Computer Science,* vol. 1, no. 1, 465–474, May 2010.

[8] S. Golemati, J. Stoitsis, E. G. Sifakis, T. Balkizas, and K.S. Nikita, "Using the Hough transform to segment ultrasound images of longitudinal and transverse sections of the carotid artery," *Ultrasound Med Biol*, vol. 33, no.12, pp. 1918–1932, Dec. 2007.

[9] J.M. Nash, J. N. Carter, and M.S. Nixon, "Dynamic feature extraction via the velocity Hough transform," *Pattern Recogn Lett*, vol. 18, no. 10, pp. 1035–1047, Oct. 1997.

[10] J. Stoitsis, S. Golemati, S. Kendros, and K.S. Nikita, "Automated detection of the carotid artery wall in B-mode ultrasound images using active contours initialized by the Hough transform," *Conf Proc IEEE Eng Med Biol Soc 2008* , vol. 2008, pp. 3146–3149.

[11] C. Xu and J.L. Prince, "Snakes, shapes and gradient vector flow," *IEEE Trans Imag Process*, vol. 7, no. 3, pp. 359–369, Mar. 1998.

[12] S. Lobregt and M.A. Viergever, "A discrete dynamic contour model," *IEEE Trans Med Imag* , vol.14, no. 1, pp. 12–24, Mar. 1995.